이학석사학위논문

효모에서 Yor289w interactome의 분석

Global analysis of Yor289w interactome in *Saccharomyces cerevisiae*

2015 년 2 월

서울대학교 대학원

생명과학부

김 지 원

효모에서 Yor289w interactome의 분석

지도교수 허 원 기

이 논문을 이학석사 학위논문으로 제출함

2015년 2월

서울대학교 대학원

생명과학부

김 지 원

김지원 의 이학석사 학위논문을 인준함

2015년 2월

위 원 장_____(인)

부위원장_____(인)

위 원_____(인)

Global analysis of Yor289w interactome in *Saccharomyces cerevisiae*

By Jiwon Kim

Advisor:

Professor Won-Ki Huh, Ph.D.

A Thesis submitted in Partial Fulfillment of the requirements for the Degree of Master of Science

February, 2015

School of Biological Sciences

Seoul National University

ABSTRACT

Identifying protein-protein interactions is essential for understanding protein function, since most cellular processes are mediated by interaction of proteins. Therefore, by identifying the interactome of a protein, we could determine the function of the protein. In this study, we conducted a genome-wide bimolecular fluorescent complementation (BiFC) assay in *Saccharomyces cerevisiae* to detect the protein-protein interactions of Yor289w and thus identify its functional role. A pRPL7B-VN-YOR289W strain and strains from a VC fusion library were mated and BiFC signals were visualized. Subsequent to BiFC screening and elimination of false positive signals, a total 56 candidates exhibited interactions with Yor289w. In the analysis of interactome, we found candidates clustered into processes related to translation initiation and nucleobase-containing small molecule metabolic processes. In addition we identified Yor289w protein expression increased in response to unfolded protein response (UPR), and that this increase was dependent on Hac1 and Ire1, which are key factors in UPR. This indicates Yor289w expression is under control of Hac1 and Ire1. On both genome-wide screening and expression data, we concluded that Yor289w might be involved in translational regulation under UPR conditions.

Key words: *YOR289W*, Protein-protein interaction, BiFC assay, *Saccharomyces cerevisiae*, Unfolded protein response (UPR).

CONTENTS

LIST OF FIGURES

LIST OF TABLES

LIST OF ABBREVIATIONS

BiFC	Bimolecular fluorescence complementation
VC	C-terminal fragment of VENUS protein
VN	N-terminal fragment of VENUS protein
GFP	Green fluorescent protein
YFP	Yellow fluorescent protein
TAP	Tandem affinity purification
UPR	Unfolded protein response
UPRE	Unfolded protein response element
DTT	Dithiothreitol
YGFLD	Yeast GFP fusion localization database
GO	Gene ontology

I. INTRODUCTION

Identifying protein-protein interactions is essential for understanding protein function. Most cellular processes are mediated by the interaction of the proteins, thus identifying the interactome of a protein can provide clues for elucidating protein function. Many methods had been developed for identifying protein-protein interactions. Such methods include yeast-two-hybrid system (Y2H) (Fields and Song, 1989; Yang et al., 1995), surface plasmon resonance (SPR) (Liedberg et al., 1983; Hiep et al., 2007), co-immunoprecipitation (Co-IP) (Phizicky and Fields. 1995), fluorescence resonance energy transfer (FRET) (Pollock and Heim 1999), and bioluminescence resonance energy transfer (BRET) (Xu et al., 1999, Pfleger and Eidne, 2006). Methods such as SPR or Co-IP are conducted in vitro, these methods do not provide information regarding the cellular localization of the protein-protein interactions, nor is it certain that the detected interactions occur in vivo. Methods such as Y2H, BRET and FRET were developed to identify in vivo protein-protein interactions. Bimolecular fluorescence complementation (BiFC) assay is an additional method developed to examine protein-protein interactions in living cells to provide more detailed information regarding localizations. The Venus fluorescent protein, which is a yellow fluorescent protein (YFP) variant, was implicated for BiFC assay (Nagai et al., 2002). In the BiFC assay the venus protein is halved, and these halved non-fluorescent fragments, VN and VC, are fused to proteins. When protein-protein interactions occur between two fused proteins, the two non-fluorescent fragments, VN and VC, are situated in close proximity and can reassemble intact fluorescent protein, thus enabling visualization of protein-protein interactions

in vivo (Kerppola, 2006; Hu et al., 2006).

The BiFC assay has been successfully utilized on *Saccharomyces cerevisiae*, and the VN fusion library for 5809 yeast open reading frames (ORFs), covering 93% of entire yeast genome was constructed (Sung et al. 2013). A VC fusion library was also constructed for genome-wide BiFC screening. Since protein-protein interactions play an important role in protein function, it is possible to predict protein function by identifying the group of proteins that have interactions with our protein of interest.

Yor289w is a putative protein of unknown function that has not been thoroughly studied. Based on previous studies, Yor289w localizes to the cytoplasm and nucleus and its abundance is approximately 1710 molecules/cell (Ghaemmaghami et al., 2003). *YOR289W* has orthologs in other eukaryotes and archaea, which contain a conserved amino acid sequence 'LRGCIG'. This sequence homology might indicate a conserved function in all these organisms. The human ortholog AMMECR1, has been the focus of a number of studies. Contiguous gene deletion in chromosome Xq22.3 results in defects such as Alport syndrome, mental retardation, midface hypoplasia, and elliptocytosis (AMME) (Vitelli et al. 1998, Tajika et al. 2005). Studies of the domain structure of AMMECR1 reveal that AMMECR1 contains a bi-layered structure domain consist a 4-stranded β-sheet, and two α-helices packed against its surfaces. This domain has been named AMMECR1 domain and orthologs including Yor289w contain this domain. Balaji named this structure the RAGNYA fold (Balaji and Aravind. 2007). *YOR289W* expression has only been analyzed by genome-wide screenings. Genome-wide microarray data indicates that *YOR289W* expression is affected by unfolded protein response (UPR) (Leber et al., 2003).

In order to study the function of Yor289w, we first examined the cellular expression and localization of GFP tagged Yor289w strains. Subsequent to determining protein localization, we conducted genome-wide BiFC screening of Yor289w, and after eliminating self-assembly candidates we identified Yor289w interactome consists of 56 proteins. The results of the interactome analysis indicate that Yor289w might play a functional role in translation initiation, nucleic acid binding and nucleobase-containing small molecule metabolic processes. The unfolded protein response (UPR) thought to affect YOR289W, was also examined. Protein expression levels of Yor289w under unfolded protein stress were assayed, and mRNA levels correlated with protein expression levels.

II. MATERIALS AND METHODS

1. Yeast strains and growth media

Yeast strains used in this study are listed in table 1. All *S.cerevisiae* strains were derived from BY4741 (MATa his3Δ1 leu2Δ0 met15Δ0 ura3Δ0) and BY4742 (MATα his3Δ1 leu2Δ0 lys2Δ0 ura3Δ0). Yeast cells were grown at 30°C in YPD (1% yeast extract, 2% glucose, 2% peptone), medium or synthetic complete medium (SC; 0.67% yeast nitrogen base without amino acids) (Sherman, 2002). Yeast strains were genetically modified according to the one-step PCR-mediated gene targeting procedure (Longtine et al., 1998). Subsequent to genetic modification proper integration was confirmed by colony-PCR method. Deletion strains were obtained from the *S.cerevisiae* deletion library (EUROSCARF) and further modifications of these strains were also conducted using the one-step PCR-mediated gene targeting procedure.

2. Transformation of yeast cells for *YOR289W* analysis

Yor289w proteins tagged with GFP, VC, VN and TAP were obtained by transformation. Yeast cells were grown to OD_{600} 0.7 in YPD medium and transformation was performed using the lithium acetate method (Gietz et al., 1995). Transformed yeast cells were plated onto SC-His, SC-Leu or SC-Ura solid medium according to the selection marker used and incubated at 30°C for 3days. Subsequent to transformation, proper integration of the tags was confirmed using the colony-PCR method. Vectors were also introduced using the lithium acetate method and selected according to their selection markers

Table1. Strains used in this study

Strain	Genotype	Source
BY4741	*MATa his3Δ1 leu2Δ0 met15Δ0 ura3Δ0*	Research Genetics
BY4742	*MATα his3Δ1 leu2Δ0 lys2Δ0 ura3Δ0*	Research Genetics
HY1562	*MATa his3Δ1 leu2Δ0 met15Δ0 ura3Δ0 HIS3MX6 YOR289W-GFP*	This study
HY1563	*MATa his3Δ1 leu2Δ0 met15Δ0 ura3Δ0 HIS3MX6 YOR289W-VN*	This study
HY1564	*MATα his3Δ1 leu2Δ0 lys2Δ0 ura3Δ0 LEU2 YOR289W-VC*	This study
HY1565	*MATa his3Δ1 leu2Δ0 met15Δ0 ura3Δ0 HIS3MX6 pRPL7b-GFP-YOR289W*	This study
HY1566	*MATa his3Δ1 leu2Δ0 met15Δ0 ura3Δ0 HIS3MX6 pRPL7B-VN-YOR289W*	This study
	MATa his3Δ1 leu2Δ0 met15Δ0 ura3Δ0 hac1Δ::kanMX6	EUROSCARF
	MATa his3Δ1 leu2Δ0 met15Δ0 ura3Δ0 ire1Δ::kanMX6	EUROSCARF
HY1567	*MATa his3Δ1 leu2Δ0 met15Δ0 ura3Δ0 hac1Δ::kanMX6 YOR289W-TAP KlURA*	This study
HY1568	*MATa his3Δ1 leu2Δ0 met15Δ0 ura3Δ0 ire1Δ::kanMX6 YOR289W-TAP KlURA*	This study
HY1569	*MATa his3Δ1 leu2Δ0 met15Δ0 ura3Δ0 YOR289W-TAP KlURA*	This study

Table 2. Plasmids used in this study

Plasmid	Genotype	Source
HB0033	pFA6a-VN173-HIS3MX6	This study
HB0055	pFA6a-HIS3MX6-pRPL7B-VN173	This study
HB0056	pFA6a-HIS3MX6-pRPL7B-VC155	This study
HB0061	pFA6a-HIS3MX6-pRPL7B-GFP	This study
HB0077	pFA6a-GFP-KlURA	This study
HB0078	pFA6a-TAP-KlURA	This study
HB0172	pFA6a-VC-LEU2	This study

Table 3. Primers used in this study

Primer	Sequence
YOR289W F2	TTATGAGGAATTTAACAAACAGTTAAAAGATATAGAGGCTG GTCGACGGATCCCCGGGTT
YOR289W R1	TTTTTTAATGTTTCTAAGACTAACTAACGAGGGTTATTTTT CGATGAATTCGAGCTCGTT
YOR289W F4	CGTCAATTTGTATCCAGATAAGATCCTTTGAAAAGATGGTG AAATCGAGCTCGTTTAAAC
YOR289W R5	TTGCAAAAAAAACTGGATTTTCGAAATAGCCTTAAAGCCAT ACCACCAGAACCTTTGTATAGTTCATCCATGC
YOR289W R5-VC	TTGCAAAAAAAACTGGATTTTCGAAATAGCCTTAAAGCCAT ACCACCAGAACCCTTGTACAGCTCGTCCATG
YOR289W R5-VN	TTGCAAAAAAAACTGGATTTTCGAAATAGCCTTAAAGCCAT ACCACCAGAACCCTCGATGTTGTGGCGGATC
YOR289W 563	TTATGCCTGAGCAACATTGG
YOR289W 723R	TTCCTCATAAGTTATGGAAC
ACT1 CHK	TGACTGACTACTTGATGAAG
ACT1 1105R	ACAGAAGGATGGAACAAAGC

3. Microscopic analysis

Yeast cells were grown to mid-logarithmic phase at 30°C in SC medium and transferred into 96-well glass bottom microplates (Matrical Bioscience, MGB096). Cells containing vectors were grown to mid-logarithmic phase at 30°C in SC-HL medium. Microscopic analysis was performed on a Nikon Eclipse E1 microscope with a Plan Fluor 100x/1.30 NA oil immersion objective lens.

4. Western blot analysis

Yeast cells grown to mid-logarithmic phase in YPD or SC medium were harvested, washed twice with phosphate-buffered saline, and disrupted by bead beating in lysis buffer (50 mM Tris-Cl, pH 7.5 150 mM NaCl, 0.15% NP-40, 1 mM EDTA) with protease inhibitors (10 mM phenylmethylsulfonyl fluoride, 1 mM benzamidine, 1 mM leupeptin, 1 mM peptistatin). Cell debris were removed by centrifugation at 13,000 rpm for 10 minute. Subsequent to centrifugation, supernatants were mixed with SDS-polyacrylamide gel electrophoresis sampling buffer, and heated at 95 for 5 minute. The supernatants were then subjected to SDS-PAGE and western blot analysis. Western blot analysis was conducted using standard methods with HRP-conjugated anti-GFP antibody (Sigma), HRP conjugated anti-mouse IgG and anti-hexokinase antibody (United States Biological).

5. Real-Time PCR analysis.

Yeast cells were grown to mid-logarithmic phase and cells were centrifuged at 2500 rpm for 5 minutes at 4°C. The supernatants were removed and yeast lysis buffer 1 (Y1 buffer) (1 M sorbitol, 0.1 M EDTA, pH 7.4), 0.1 mg/ml zymolase, and 0.1% mercaptoethanol were added. Cells were incubated at 30°C for 30 minute and then yeast mRNA was extracted using the RNeasy Mini Kit (Qiagen). Subsequent to RNA sample preparation, whole samples were diluted with RNase free water to a concentration of 10 µg/ml. cDNA was gained by reverse transcription using the M-MLV reverse transcriptase (Mbiotech). YOR289W 563, and YOR289W 723R primers were used for quantitative real-time PCR analysis. The *ACT1* was used as control for each experiment. The *ACT1* primers ACT1-CHK, and ACT1-1153 were used. Amplification and detection were performed with the SensiFAST SYBR Hi-ROX mixture (Bioline) using a 7300 Real Time PCR system (Applied Biosystems). The cycle threshold (Ct) values of *YOR289W* and *ACT1* were analyzed; the *YOR289W* Ct value was normalized to the *ACT1* Ct value and the resulting value was used as a measurement of the relative amount of *YOR289W* mRNA.

III. RESULTS

1. Identification of Yor289w expression and cellular localization

The initial approach for elucidating the cellular function of Yor289w was to identify its cellular localization. The GFP tag was amplified by PCR using the pFA6a-GFP-His3MX6 vector as template and primers YOR289W F2 and YOR289W R1. Using this process we constructed a C-terminally GFP tagged Yor289w strain. In addition, the pFA6a-His3MX6-pRPL7B-GFP vector was used as template together with primers YOR289W F4 and YOR289W R5 to generate an N-terminally GFP tagged Yor289w strain. Both strains were used to determine the cellular localization and expression level of Yor289w. The N-terminally GFP tagged strain was under control of an RPL7B promoter, while the C-terminally GFP tagged Yor289w was under the control of its native promoter. N-terminally GFP tagged Yor289w protein was detected on both western blot analysis and microscopic analysis. The microscopic assay indicates that Yor289w is localized to the cytoplasm and nucleus (Figure 1A). Both western blot and microscopic analysis exhibit lower Yor289w expression under control of the native promoter than under the RPL7B promoter (Figure 1B).

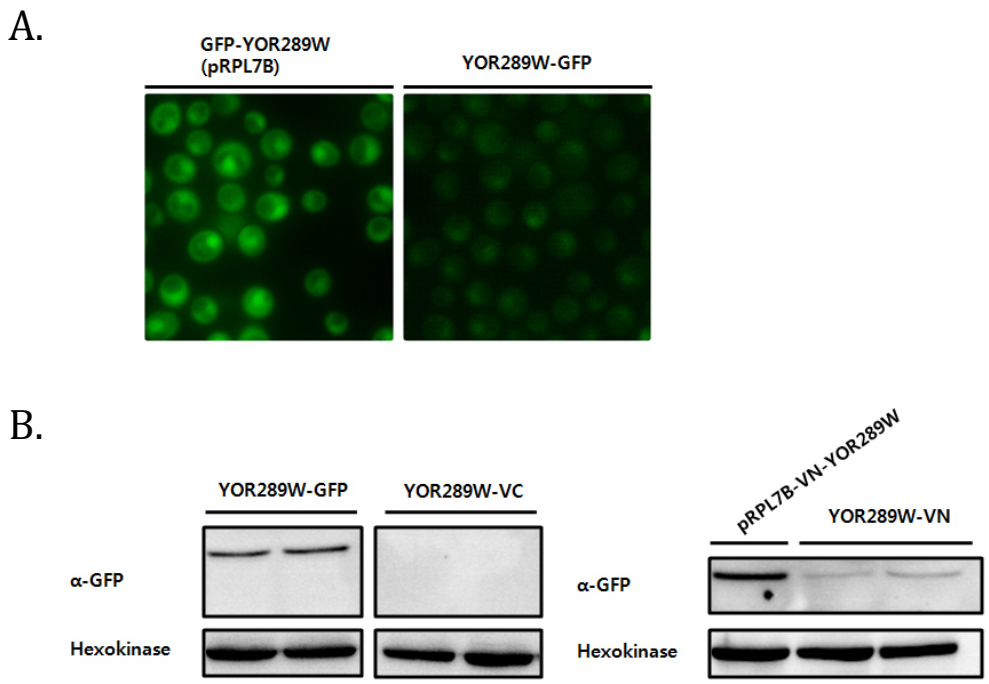

Figure 1. Yor289w protein localization and expression

(A) The Yor289w GFP fusion proteins were detected by microscopic assay. The N-terminally GFP tagged strain was expressed under the control of an RPL7B promoter and the C-terminally GFP tagged strain was expressed under the control of the native *YOR289W* promoter. Expression under the native promoter was lower; however nucleus and cytoplasm localization was still detectable. (B) Yor289w tagged with either GFP or VN was detected by western blot analysis. The expression level under the RPL7B promoter was higher than under the native promoter similar to the result of the microscopic assay. The N-terminally VN tagged strain was used for genome-wide BiFC screening.

2. Identification of the Yor289w interactome.

2-1. Genome-wide mating and selection for microscopic analysis

Yor289w expression under its native promoter is low, as established using the microscopic assay. Therefore expressing Yor289w under RPL7B promoter was used for further microscopic assays. In order to identify the Yor289w interactome, we conducted genome-wide BiFC screening. VN and VC tagged Yor289w strains were constructed and the expression of VN and VC tagged Yor289w was analyzed by western blot analysis. VC tagging was not detected by western blot analysis for unknown reasons (Figure 1B). The VN tagged strain was well-expressed as determined by western blot analysis and was therefore used for further analysis. The pRPL7B-VN-YOR289W mating type a strain was mated with the entire VC library mating type α then plated and selected on SC-HL plates. Subsequent to selection, cells were used for BiFC assay (Figure 2A).

2-2. Genome-wide BiFC screening of Yor289w and elimination of self-assembly candidates

Of the strains tested microscopically, 176 strains exhibited BiFC signals. BiFC signals included nucleus, cytoplasm, bud neck, ER, cell periphery, and punctuate localizations. However these signals could include interaction between the VN and VC tags as well as protein interactions between Yor289w and its target proteins. To eliminate these false-positive interactions, strains containing VN tag under the control of the RPL7B promoter was constructed and also mated for genome-wide screening (Figure 2A). Screening for self-assembly resulted in candidates, 434 candidates with YFP signals. Of the 176

A.

<YOR289W screening>

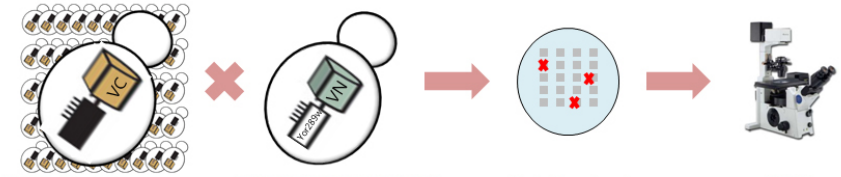

<Self-assembly screening>

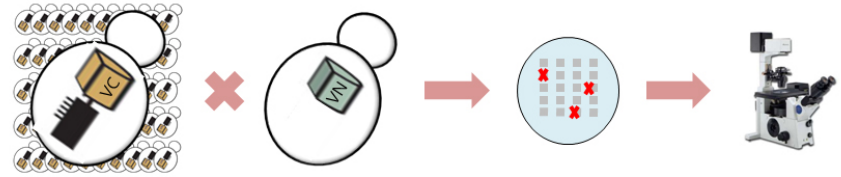

B.

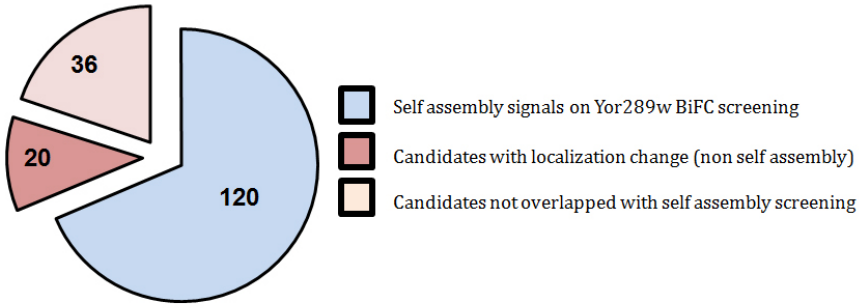

- 434 signals detected on pRPL7B-VN screening (Self assembly)
- 176 signals detected on YOR289W screening
- Total 56 signals were identified as interactome of Yor289w

Figure 2. Genome-wide BiFC screening of Yor289w

(A) Diagram for genome-wide BiFC screening. The pRPL7B-VN-YOR289W strain was constructed for genome-wide BiFC screening and mated with the VC fusion library strains. For self-assembly screening, a strain expressing only the VN tag was constructed and mated with the VC fusion library. Subsequent to mating diploid cells were selected for microscopic assay. (B) Results of the genome-wide BiFC screening. In total, 176 BiFC signals were detected on YOR289W screening. Of these signals, 120 signals were found to be self-assembly signals, and 56 signals were identified as signals derived from protein-protein interactions.

Table 4. Yor289w genome-wide BiFC screening results

Standard name	Localization on BiFC	Localization from YGFLD	Self assembly check(N/C)
RNR1	PUNCTATE	ambiguous	C
URA7	PUNCTATE	cytoplasm	C
CYS4	PUNCTATE	cytoplasm	C
GLK1	PUNCTATE	cytoplasm,punctate composite	C
FPR4	PUNCTATE	nucleolus,nucleus	C
GVP36	PUNCTATE	cytoplasm	C
BMH1	PUNCTATE	cytoplasm	C
SEC27	PUNCTATE	Golgi,early Golgi	C
ZRC1	PUNCTATE	vacuolar membrane	C
SEC13	PUNCTATE	ER to Golgi	C
VMA10	PUNCTATE	vacuolar membrane	C
SEC72	PUNCTATE	ER	C
SEC31	PUNCTATE	ER to Golgi	N
RPA135	NUCLEOLUS	nucleolus	N
ADE3	NUCLEUS, CYTOPLASM	cytoplasm,nucleus	N
PWP2	NUCLEOLUS	nucleolus	N
HSP104	NUCLEUS	cytoplasm	N
GCD6	PUNCTATE	cytoplasm	N
GSY2	PUNCTATE	cytoplasm,nucleus,punctate composite	N
TEF4	CYTOPLASM	cytoplasm	N
ADE4	PUNCTATE	cytoplasm	N
ENO1	NUCLEUS, CYTOPLASM	cytoplasm	N
MAP1	PUNCTATE	cytoplasm,nucleus	N
GCD7	PUNCTATE	cytoplasm,punctate composite	N
HEK2	PUNCTATE	cytoplasm	N
HSP42	PUNCTATE	cytoplasm	N
CPR6	NUCLEUS, CYTOPLASM	cytoplasm	N
PDR16	PUNCTATE	lipid particle	N
RPS4B	PUNCTATE	cytoplasm	N
MET22	PUNCTATE	cytoplasm,nucleus	N
MTQ1	NUCLEUS, CYTOPLASM	mitochondrion	N

YLR257W	PUNCTATE	cytoplasm	N
GIC1	NUCLEUS, CYTOPLASM	cytoplasm,nucleus	N
SOL2	PUNCTATE	cytoplasm	N
SBP1	PUNCTATE	cytoplasm	N
YDR535C	NUCLEUS, CYTOPLASM	0	N
PET18	PUNCTATE	ambiguous	N
EGD2	CYTOPLASM	cytoplasm	N
GIS2	PUNCTATE	cytoplasm	N
RPS22A	PUNCTATE	nucleolus,nucleus	N
MBF1	PUNCTATE	cytoplasm	N
RPL41A	CYTOPLASM	cytoplasm	N
TOM70	MITOCHONDRIA	mitochondrion	N
HXT3	CELL WALL	cell periphery,vacuole	N
VMA2	NUCLEOLUS, PUNCTATE	vacuolar membrane	N
LCB1	PUNCTATE	ER	N
PEX11	PUNCTATE	peroxisome	N
YOP1	PUNCTATE	ER	N
ADE5,7	NUCLEUS	cytoplasm	C
MET6	NUCLEUS, CYTOPLASM	cytoplasm	C
SSE1	NUCLEUS, CYTOPLASM	cytoplasm	C
ADE17	NUCLEUS, CYTOPLASM	cytoplasm	C
LPX1	NUCLEUS, CYTOPLASM	ambiguous	C
SAM1	NUCLEUS, CYTOPLASM	cytoplasm	C
SAM2	NUCLEUS, CYTOPLASM	ambiguous	C
PSA1	NUCLEUS, CYTOPLASM	cytoplasm	C

The self-assembly check refers to a signal resulting from self-assembly. N stands for non self-assembly candidates and C stands for chang in localization identified by the BiFC assay.

strains demonstrating signals in the Yor289w BiFC screening, 140 strains overlapped with the self-assembly screening. Of the 140 overlapping candidates, 26 candidates demonstrated changes to the localization of their YFP signals; a difference in localization between signals was considered as an interaction. Using this process we identified 62 possible candidates that interact with Yor289w.

Additional measure was taken to eliminate false positive signals. Yor289w expression in the pRPL7B-GFP-YOR289W strain was localized to the nucleus and cytoplasm (Figure 1A). While the VN tags expressed under RPL7B promoter did not exhibit cellular localization, therefore we could assume VN tags were distributed throughout the nucleus and cytoplasm at equal levels. Since the signals from pRPL7B-GFP-YOR289W strain were more intense in the nucleus, this could indicate that these are self-assembly signals. To eliminate these self-assembly candidates, candidates demonstrating change in localization were examined. Candidates demonstrating localization in the cytoplasm and nucleus, and corresponding self-assembly signals in the cytoplasm, were removed from the interactome list. By this processes a total 56 proteins were identified as the interactome, which had higher probability of physical interaction with Yor289w (Figure 2B) (Table 4).

2-3. Functional analysis of the Yor289w interactome

The interactome candidates were categorized according to the fluorescent signal type. 36 candidates demonstrated punctate localization signals, 22 demonstrated nucleus signals, three demonstrated cytoplasm signals, one demonstrated mitochondria signal, one demonstrated cell periphery signal,

and the remaining candidate demonstrated other type of signal. Most of the punctate localized candidates were originally cytoplasm localized proteins according to Yeast GFP Fusion Localization Database (YGFLD).

To further elucidate the functional role and involvement of Yor289w, the processes in which 56 Yor289w interactome candidates are involved were further analyzed using the Saccharomyces Genome Database (SGD), SGD Gene Ontology (GO) Slim Mapper. Of the 56 proteins, 10 (17.9%) were involved in process annotated as nucleobase-containing small molecule metabolic process. Seven proteins were involved in cellular amino acid metabolic process and six proteins were involved in carbohydrate metabolic process (Table 5). To confirm which of these processes were functionally related to Yor289w, we analyzed the p-value of each process. A p-value <0.01 was obtained for the nucleobase-containing small molecule metabolic process, regulation of translation, protein folding, cellular amino acid metabolic process, and carbohydrate metabolic process. These processes were therefore thought to have functional association with Yor289w (Table 6).

Another approach used for analyzing the Yor289w interactome was GeneMANIA prediction. This method analyzes the interactome by functional similarity and interactions. The databases used for this analysis include GEO, BioGRID, Pathway Commons, and I2D. One feature of GeneMANIA is the addition of non-query genes based on weight of interaction as determined by a Gaussian field label propagation algorithm. This analysis allows for the visualization of network on Yor289w interactome. The visualized interaction network demonstrated the physical interaction between interactome and non-query genes that have significant interactions with the interactome (Figure 3A.) (Warde-Farley et al., 2010; Montojo et al., 2014). Using this approach we were

Table 5 . Interactome analysis using SGD GO-slim mapper.

GO term	Candidate Frequency	Genome Frequency	Genes
Nucleobase-containing small molecule metabolic process	10 out of 56 genes, 17.9%	226 of 6337 genes, 3.6%	URA7,PSA1,SAM2,RNR1, ADE5,7,ADE3,SAM1, SEC13,ADE17,ADE4
Cellular amino acid metabolic process	7 out of 56 genes, 12.5%	242 of 6337 genes, 3.8%	SAM2,MET6,CYS4,ADE3, SAM1,ZRC1,MET22
Carbohydrate metabolic process	6 out of 56 genes, 10.7%	267 of 6337 genes, 4.2%	GLK1,PSA1,BMH1,ENO1, HSP104,GSY2
Regulation of organelle organization	5 out of 56 genes, 8.9%	247 of 6337 genes, 3.9%	BMH1,ENO1,GIC1,FPR4, PDR16
Lipid metabolic process	5 out of 56 genes, 8.9%	276 of 6337 genes, 4.4%	URA7,LCB1,PDR16, PEX11,LPX1
Regulation of translation	5 out of 56 genes, 8.9%	95 of 6337 genes, 1.5%	GCD6,SBP1,GCD7,MTQ1, GIS2
Regulation of cell cycle	4 out of 56 genes, 7.1%	193 of 6337 genes, 3.0%	BMH1,CYS4,GIC1,PDR16
Transmembrane transport	4 out of 56 genes, 7.1%	227 of 6337 genes, 3.6%	VMA2,HXT3,SEC72, TOM70
Protein folding	4 out of 56 genes, 7.1%	94 of 6337 genes, 1.5%	EGD2,HSP104,CPR6, SSE1
Generation of precursor metabolites and energy	4 out of 56 genes, 7.1%	158 of 6337 genes, 2.5%	GLK1,BMH1,ENO1,GSY2
Organelle fission	4 out of 56 genes, 7.1%	282 of 6337 genes, 4.5%	BMH1,GIC1,PDR16, PEX11
Cytoskeleton organization	3 out of 56 genes, 5.4%	239 of 6337 genes, 3.8%	HSP42,GIC1,GVP36
Protein targeting	3 out of 56 genes, 5.4%	275 of 6337 genes, 4.3%	EGD2,SEC72,TOM70
Protein complex biogenesis	3 out of 56 genes, 5.4%	325 of 6337 genes, 5.1%	VMA2,FPR4,YOP1
Cellular ion homeostasis	3 out of 56 genes, 5.4%	123 of 6337 genes, 1.9%	VMA2,VMA10,ZRC1
Monocarboxylic acid metabolic process	3 out of 56 genes, 5.4%	125 of 6337 genes, 2%	GLK1,ENO1,PEX11
Mitotic cell cycle	3 out of 56 genes, 5.4%	322 of 6337 genes, 5.1%	BMH1,CYS4,GIC1
Cofactor metabolic process	3 out of 56 genes, 5.4%	133 of 6337 genes, 2.1%	SAM2,ADE3,SAM1

Cytoplasmic translation	3 out of 56 genes, 5.4%	171 of 6337 genes, 2.7%	RPL41A,RPS4B,RPS22A
Golgi vesicle transport	3 out of 56 genes, 5.4%	190 of 6337 genes, 3%	SEC31,SEC27,SEC13

Table 6. Processes evaluated by p-value.

Process	**p-value (<0.01)**	**Candidates**
Nucleobase-containing small molecule metabolic process	4.043.E-09	URA7,PSA1,SAM2,RNR1,ADE5,7, ADE3,SAM1,SEC13,ADE17,ADE4
Regulation of translation	2.024.E-06	GCD6,SBP1,GCD7,MTQ1,GIS2
Protein folding	2.296.E-04	EGD2,HSP104,CPR6,SSE1
Cellular amino acid metabolic process	1.349.E-03	SAM2,MET6,CYS4,ADE3,SAM1,FPR4, ZRC1,MET22
Carbohydrate metabolic process	7.726.E-03	GLK1,PSA1,BMH1,ENO1,HSP104, GSY2

able to identify clusters of genes that involved in particular cellular process. The false discovery rate (FDR) of the cluster candidates was determined, and clusters with an FDR value <0.01 were considered to have a functional association with Yor289w (Table 7).

The associated clusters with the lowest FDR values included translation factor activity, nucleic acid binding, translation initiation factor activity, posttranscriptional regulation of gene expression, regulation of translation, nucleobase-containing small molecule metabolic process, and purine-containing compound metabolic process. These clusters could be divided into two groups; one containing *GCD6, GCD7, GIS2, MTQ1*, *HEK2,* and *SBP1* and the other containing *ADE3, ADE4, ADE5,7, ADE17, PSA1, RNR1, SAM1, SAM2*, *SEC13,* and *URA7*. The latter group is involved in nucleobase-containing small molecule metabolic process, purine-containing compound metabolic process (Figure 3C) and the former group was involved in the other processes mentioned (Figure 3B). Other clusters identified by GeneMANIA analysis included ER to Golgi transport vesicle membrane and vesicle coat which involve *SEC13, SEC27* and *SEC31* as core proteins (Figure 3D). Processes related to translation and gene expression scored lower. The proteins involved in this interaction network included *GCD6, GCD7, GIS2, MTQ1, HEK2,* and *SBP1* as well as *GCD6* and *GCD7* that form core with *GCD1, GCD2* and *GCN3*, which was are not part of the Yor289w interactome. These proteins form the eukaryotic initiation factor 2B (eIF2B) complex that function as a guanine-nucleotide exchange factor essential for protein synthesis initiation (Graham et al. 1998). Yor289w might play a role in this process since the core protein physically interacts with Yor289w. Yor289w might also have a functional association with other processes identified by GeneMANIA as having a low FDR value (Table 7).

Table 7 . Interactome analysis using GeneMANIA.

Feature	FDR	Genes in network	Genes in genome	Genes in candidates	Expanded candidates
Translation factor activity, nucleic acid binding	2.05E-04	8	44	GCD6, GCD7, TEF4	GCD1, GCD2, GCN3, SUI3
Translation initiation factor activity	1.79E-03	6	29	GCD6, GCD7	GCD1, GCD2, GCN3, MRF1, SUI4
Posttranscriptional regulation of gene expression	1.79E-03	10	116	GCD6, GCD7, GIS2, MTQ1, HEK2, SBP1	GCD1, GCD2, GCN3, EFB1
Regulation of translation	1.87E-03	9	93	GCD6, GCD7, GIS2, MTQ1, SBP1	GCD1, GCD2, GCN3, EFB1
Nucleobase-containing small molecule metabolic process	2.12E-03	12	190	ADE3, ADE4, ADE5,7, ADE17, PSA1, RNR1, SAM1, SAM2, SEC13, URA7	ADE16, SEC23
Purine-containing compound metabolic process	2.12E-03	9	99	ADE4, ADE5,7, ADE17, SAM1, SAM2, SEC13	ADE16, SEC23
Regulation of translational initiation	3.20E-03	5	21	GCD6, GCD7	GCD1, GCD2, GCN3
Guanyl-nucleotide exchange factor activity	5.47E-03	6	42	GCD6, GCD7	GCD1, GCD2, GCN3, EFB1
ER to Golgi transport vesicle membrane	5.47E-03	4	12	SEC13, SEC31	SEC23, SEC24
Regulation of cellular protein metabolic process	5.47E-03	11	184	GCD6, GCD7, GIS2, BMH1, FPR4, MTQ1, SBP1	GCD1, GCD2, GCN3, EFB1
Regulation of protein metabolic process	7.46E-03	11	192	GCD6, GCD7, GIS2, BMH1, FPR4, MTQ1, SBP2	GCD1, GCD2, GCN3, EFB1
Translational initiation	1.38E-02	6	51	GCD6, GCD7	GCD1, GCD2, GCN3, SUI3

Genes in network: the total number of genes identified by GeneMANIA, Genes in genome: the number of whole genes involved in each process. Gene names in the clusters are listed in the fifth and sixth columns.

A.

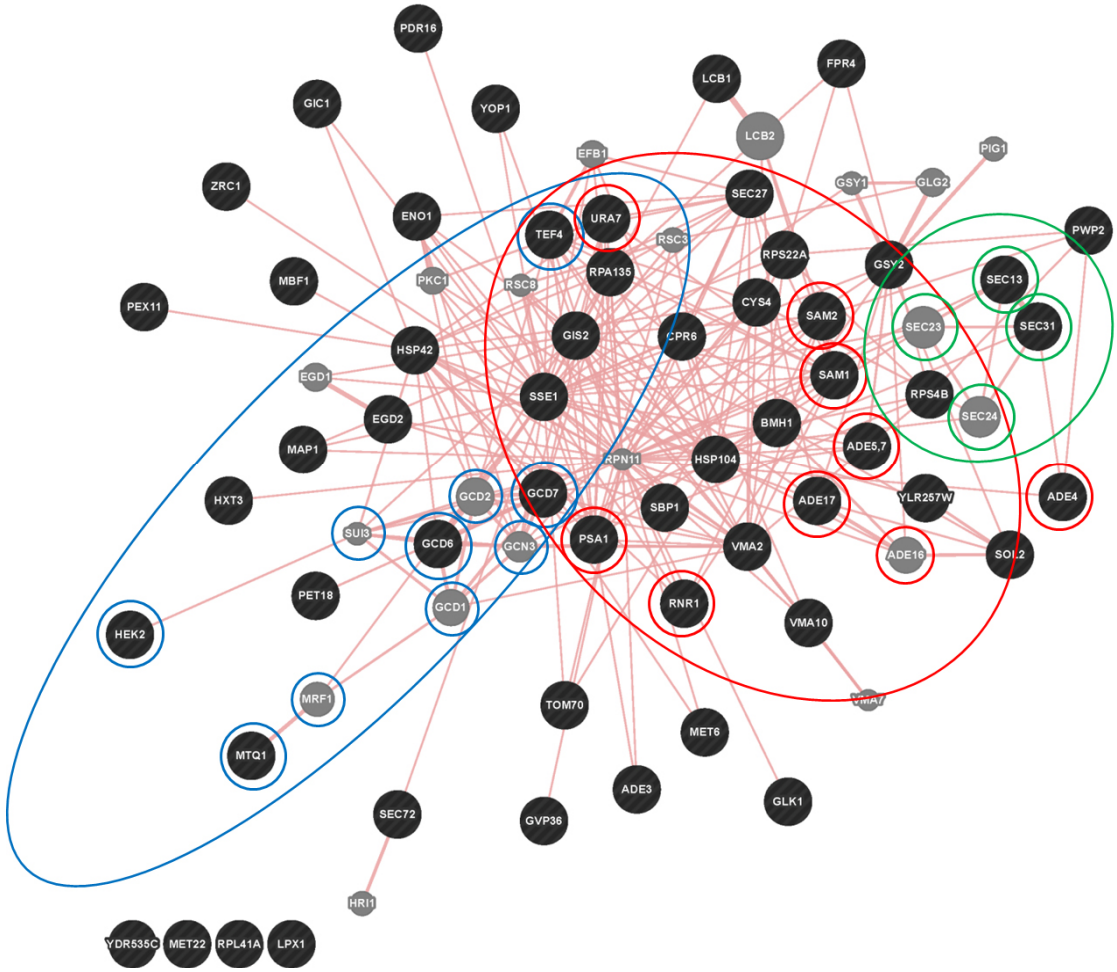

GCD6, GCD7, HEK2, TEF4, MTQ1

- Translation factor activity
- Nucleic acid binding
- Translation initiation factor activity
- Posttranscriptional regulation of gene expression
- Regulation of translation

SEC13, SEC31

- ER to Golgi transport vesicle membrane

ADE3, ADE4, ADE17, ADE5,7, RNR1, SAM1, SAM2, URA7, PSA1,SEC13,

- Nucleobase-containing small molecule metabolic process
- Purine-containing compound metabolic process

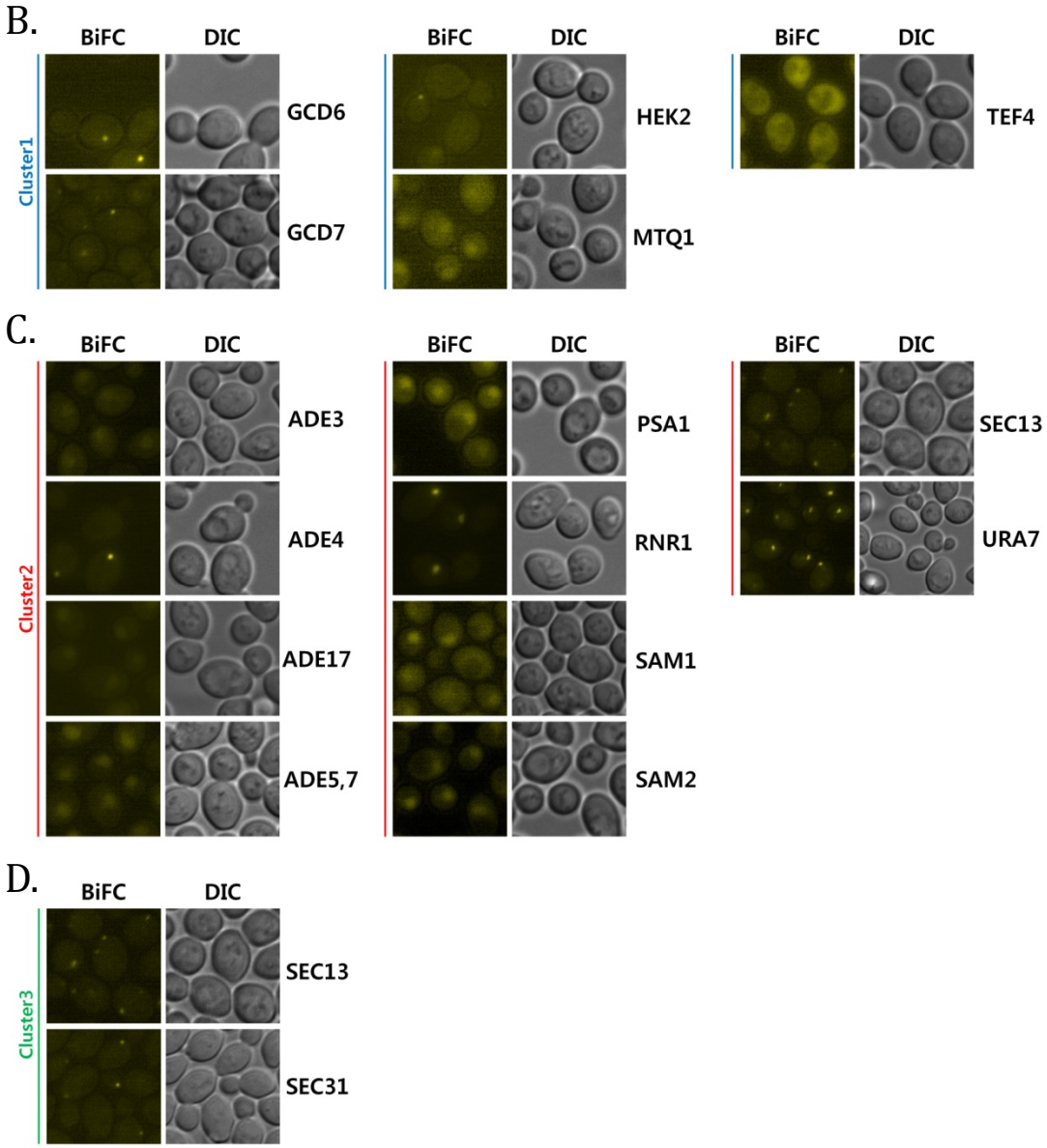
B.
BiFC
DIC
Cluster1
GCD6
GCD7
HEK2
MTQ1
TEF4
C.
Cluster2
ADE3
ADE4
ADE17
ADE5,7
PSA1
RNR1
SAM1
SAM2
SEC13
URA7
D.
Cluster3
SEC13
SEC31

Figure 3. Result of GeneMANIA analysis

(A) The protein-protein interaction network of the Yor289w interactome and clusters. The 56 proteins identified in this study are in black and proteins with clustering interaction that are not part of the interactome are in gray. Three circles colored blue, red, and green indicate the clusters with low false discovery rate (FDR) scores. *GDC6* and *GCD7* constitute the interaction core for translation factor activity, nucleic acid binding, translation initiation factor activity, posttranscriptional regulation of gene expression, and regulation of translation. Protein-protein interactions involved in nucleobase-containing small molecule metabolic process and purine-containing compound metabolic process shown to be interrelated. *SEC13*, and *SEC31* that comprise the COPII vesicle coat have scored low FDR score. (B) BiFC signals of candidates that cluster with translation factor activity, nucleic acid binding, translation initiation factor activity, posttranscriptional regulation of gene expression, and regulation of translation. (C) BiFC signals of candidates that cluster with nucleobase-containing small molecule metabolic process and purine-containing compound metabolic process. (D) BiFC signals of candidates that cluster with ER to Golgi transport vesicle membrane.

3. Yor289w protein expression under stress conditions

Prior microarray screening data that *YOR289W* might be affected by the unfolded protein response (UPR) (Leber et al., 2004), therefore we tested the expression of Yor289w under stress conditions including osmotic stress, heat stress, and unfolded protein stress (Figure 4A).

3.1 Dithiothreitol and tunicamycin treatment induce expression of Yor289w.

A previous study suggested that UPR induces transcription factor HAC1,and that Hac1 binds to specific conserved sequence called unfolded protein response elements (UPRE). These sequences can be divided into three types of UPRE. There were UPRE1, UPRE2, and UPRE3 (Patil and Walter, 2004). The promoter region of *YOR289W* contains an UPRE2 sequence located 183bp upstream of the start of the transcription. Suggesting an association with UPR. Since the possible association between UPR and Yor289w is intriguing (Travers et al., 2000; Leber et al., 2004), we first tested Yor289w expression under UPR conditions.

Dithiothreitol (DTT) is a reducing agent that acts on protein folding. DTT can cross membranes and prevent disulfide formation, thus inducing protein misfolding (Rubio et al., 2011)., Yor289w expression was up-regulated by the treatment of 5 mM DTT, as determined by western blot analysis (Figure 4A),indicating that Yor289w expression might be affected by UPR.

As Yor289w protein expression showed significant increase on DTT treatment, we tried to define if Yor289w level was affected by UPR. Tunicamycin is a mixture of homologous nucleoside antibiotics that blocks N-linked

glycosylations, thereby inducing UPR on mechanism different from DTT (Travers et al., 2000). Experiment done under 2 μg of tunicamycin, we could detect YOR289W protein fold-increase. Since both UPR inducing agents showed significant protein level increase, we could conclude that UPR induces Yor289w level increase (Figure 4B).

Since Yor289w protein levels were affected by UPR inducing conditions, we examined whether other types of stress also resulted in up-regulation of Yor289w expression. Osmotic stress was induced by treatment with 1M NaCl, and heat stress was induced by incubating cells at the 37°C. Yor289w protein levels increased upon induction of heat stress but were unaffected by other stress conditions. However, as the effect of the heat stress was not as significant as that of UPR we choose to focus on UPR stress.

3.2 The Hac1 transcription factor controls the expression of *YOR289W* under UPR inducing conditions.

UPR induction involves two factors that regulate UPR target genes. *HAC1* encodes a basic leucine zipper (b-zip) transcription factor controlling UPR target genes and its mRNA contains an intron. *IRE1* encodes an ER-resident transmembrane serine-threonine kinase and endoribonuclease which mediates UPR. In the presence of the UPR inducing conditions, Ire1 dimerizes and endonuclease activity is induced. Ire1 eventually cleaves the intron of *HAC1* mRNA and enabling translation. Translated Hac1 acts as a transcription factor and induces expression of UPR target genes (Nojima et al., 1994; Patil and Walter, 2001; Mori, 2009). The protein levels of Yor289w were tested in wild-type (WT) and *HAC1* and *IRE1* deletion strains. The Yor289w protein levels were increase upon DTT and tunicamycin

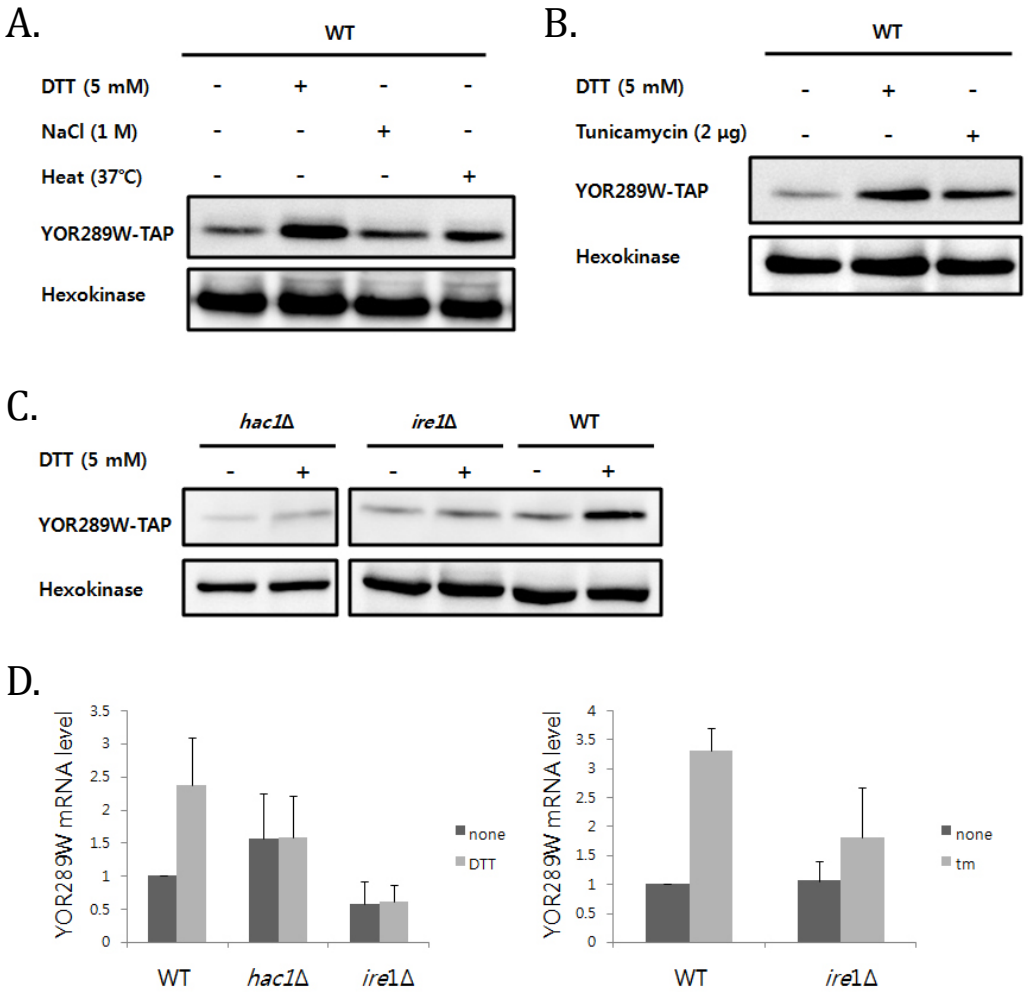
A.
WT
DTT (5 mM) - + - -
NaCl (1 M) - - + -
Heat (37℃) - - - +
YOR289W-TAP
Hexokinase
B.
WT
DTT (5 mM) - + -
Tunicamycin (2 μg) - - +
YOR289W-TAP
Hexokinase
C.
hac1Δ
ire1Δ
WT
DTT (5 mM) - + - + - +
YOR289W-TAP
Hexokinase
D.
YOR289W mRNA level
3.5
3
2.5
2
1.5
1
0.5
0
none
DTT
WT
hac1Δ
ire1Δ
YOR289W mRNA level
4
3.5
3
2.5
2
1.5
1
0.5
0
none
tm
WT
ire1Δ

Figure 4. Yor289w expression affected by unfolded protein stresses

(A) Yor289w level was affected by stress. Yor289w protein levels were analyzed using the YOR289W-TAP stain with DTT, NaCl and heat induction. DTT treatment resulted in significant increase in Yor289w protein levels. Osmotic stress did not induce protein expression and heat stress induced protein expression at a lower level than treatment with DTT. (B) Yor289w levels increase under ER misfolding stresses. DTT and tunicamycin treatment were used to induce ER protein misfolding, thereby activating UPR. (C) UPR controls the expression of Yor289w. *hac1*Δ and *ire1*Δ strains showed did not demonstrated an increase in Yor289w expression in response to DTT treatment. This indicates that Yor289w expression is dependent on the Hac1 transcription factor. (D) The effect of DTT and tunicamycin treatment on *YOR289W* mRNA expression. Wild type cells exhibited an increase in *YOR289W* mRNA levels as a result of treatment. The *hac1*Δ and *ire1*Δ strain did not demonstrate a significant increase in expression in response to either treatment.

treatment, but were unaffected in the *hac1*Δ and *ire1*Δ strains as demonstrated by western blot analysis (Figure 4C). This indicates that *YOR289W* is an UPR target gene regulated by the Hac1 transcription factor.

Next we examined whether the increase in Yor289w protein expression level is dependent on *YOR289W* mRNA expression levels. The *YOR289W* mRNA level subsequent to DTT and tunicamycin treatment was measured using the real-time PCR method and the Ct value for each experiment was analyzed. Ct values were normalized to the Ct value of *ACT1*. The result obtained were similar to those of the protein level; *YOR289W* mRNA level demonstrated approximately two fold increase subsequent to DTT and tunicamycin treatment. Increased mRNA levels were not observed on *hac1*Δ and *ire1*Δ strains (Figure 4D). These results indicate that the Yor289w protein level in response to DTT and tunicamycin treatment was due to an increase in mRNA levels caused by the induction of the unfolded protein response by these compounds. Furthermore, the absence of an increase in *YOR289W* mRNA level in the *hac1*Δ and *ire1*Δ strains indicates that *YOR289W* mRNA levels were dependent on Hac1.

IV. DISSCUSSION

In this study, a genome-wide BiFC screening of the Yor289w interactome revealed 56 possible candidates with a high probability of interaction with Yor289w, as well as identifying the localization of the interactions. Previous genome-wide screening, methods including PCA, TAP-MS and Y2H were unable to identify the Yor289w interactome (Tarassov et al,. 2008; Gavin et al., 2006, Ito et al., 2001; Uetz et al., 2000). A TAP-MS study conducted by Krogan et al. identified Jip4 and Ydr474c as possible Yor289w protein interaction partners (Krogan et al., 2006). However Jip4 and Ydr474c were not identified by the genome-wide BiFC screening. This might be due to the topology of the VN and VC fragments, masking positive BiFC interactions. Despite this limitation of BiFC, we were able to identify several interaction candidates, indicating that BiFC can be used to detect interactions not identified by other methods.

On the candidates that were found to be the interactome in this study, may still include false-positive signals. Since the Yor289w interacting domain has yet to be identified these false positive signal could not be eliminated by comparing a non-interacting form of Yor289w protein with the intact Yor289w protein using BiFC. Therefore we decided the best option was to remove self-assembly signal by the pRPL7B-VN strain.

Candidates identified by BiFC screening exhibited mainly nucleus and punctuate localization. The Yor289w protein was originally thought to localize to the nucleus and cytoplasm according to microscopic analysis of GFP tagged strains and previous data (Huh et al., 2003). However the punctate localization was not detected in our microscopic assay conducted with GFP tagged strains.

GFP tagged strains under the control of the RPL7B promoter, exhibited robust GFP signals in the nucleus; it is possible that the punctate localization signals are masked by the strong signal from nucleus. The genome-wide screening was done by VN tagged strain under control of the RPL7B promoter, protein-protein interactions manifested puntate signals but not nucleus signals. These results suggest that the puntate signal might reflect interactions between Yor289w and candidate proteins affecting the cellular localization.

The interactome analyses performed with SGD GO-Slim mapper and GeneMANIA suggested the possible involvement of the Yor289w protein in regulation of translation or eIF2B activity. Candidates that were related to this activity include *GCD6 SBP1, GCD7, MTQ1*, and *GIS2*. Of these candidates, *GCD6, SBP1, GCD7,* and *GIS2* were proteins that demonstrated punctate localization in the BiFC analysis (Figure 3B). As *GCD6* and *GCD7* are subunits of eIF2B, Yor289w might interact with these proteins to alter eIF2B activity. Since the role of eIF2B is to exchange GDP to GTP on eIF2 thereby facilitating the translation process (Teske et al., 2011), these interactions might suggest that Yor289w is involve d in regulating translation.

Another aspect we examined was the effect of cellular stresses on *YOR289W*. Present microarray data indicates that *YOR289W* might be controlled by UPR stress (Leber et al., 2003). The results of this study indicate that under UPR stress condition Yor289w protein levels increase and that this increase was dependent on Hac1 and Ire1. These results correlate with *YOR289W* mRNA levels determined by real-time PCR analysis (Figure 4). Based on these results we concluded that increased Yor289w protein expression is due to upregulation of mRNA expression under UPR stress condition and that this process is regulated by transcription factor Hac1 and endonuclease Ire1.

Yor289w might play a protein regulatory role in induction of expression by UPR. Further functional analysis aimed at identifying the exact functional role of Yor289w could examine translational initiation due to UPR or eIF2B activity during UPR. Since eIF2B represses translation initiation under stressed conditions (Teske et al., 2011), it is possible that Yor289w is involved in translation process. Previous study identified that the conserved 'LRGCIG' sequence possibly involved in DNA or RNA binding in the Yor289w cleft conformation (Balaji and Aravind. 2007), suggesting another potential role for Yor289w.

Since Yor289w overexpression in response to DTT and tunicamycin treatment was not detected in either the Hac1 or Ire1 deletion strains. Yor289w might not play a centrol role in the central role in the response to ER protein misfolding (Data not shown). Since Yor289w expression is normally low, it might play a minor role in translation regulation. Additional analysis is required to further elucidate the role of Yor289w.

V. REFERENCE

Balaji, S., & Aravind, L. (2007). The RAGNYA fold: a novel fold with multiple topological variants found in functionally diverse nucleic acid, nucleotide and peptide-binding proteins. Nucleic acids research, 35(17), 5658-5671.

Fields, S., & Song, O.-k. (1989). A novel genetic system to detect protein protein interactions.

Gavin, A.-C., Aloy, P., Grandi, P., Krause, R., Boesche, M., Marzioch, M., Dümpelfeld, B. (2006). Proteome survey reveals modularity of the yeast cell machinery. Nature, 440(7084), 631-636.

Ghaemmaghami, S., Huh, W.-K., Bower, K., Howson, R. W., Belle, A., Dephoure, N., Weissman, J. S. (2003). Global analysis of protein expression in yeast. Nature, 425(6959), 737-741.

Hu, C. D., Grinberg, A. V., & Kerppola, T. K. (2006). Visualization of protein interactions in living cells using bimolecular fluorescence complementation (BiFC) analysis. Current protocols in cell biology.

Huh, W.-K., Falvo, J. V., Gerke, L. C., Carroll, A. S., Howson, R. W., Weissman, J. S., & O'Shea, E. K. (2003). Global analysis of protein localization in budding yeast. Nature, 425(6959), 686-691.

Kerppola, T. K. (2006). Visualization of molecular interactions by fluorescence complementation. Nature reviews Molecular cell biology, 7(6), 449-456.

Krogan, N. J., Cagney, G., Yu, H., Zhong, G., Guo, X., Ignatchenko, A., Tikuisis, A. P. (2006). Global landscape of protein complexes in the yeast Saccharomyces cerevisiae. Nature, 440(7084), 637-643.

Leber, J. H., Bernales, S., & Walter, P. (2004). IRE1-independent gain control of the unfolded protein response. PLoS biology, 2(8), e235.

Liedberg, B., Nylander, C., & Lunström, I. (1983). Surface plasmon resonance for gas detection and biosensing. Sensors and actuators, 4, 299-304.

Longtine, M. S., McKenzie III, A., Demarini, D. J., Shah, N. G., Wach, A., Brachat, A., Pringle, J. R. (1998). Additional modules for versatile and economical PCR-based gene deletion and modification in Saccharomyces cerevisiae. Yeast, 14(10), 953-961.

Minh Hiep, H., Endo, T., Kerman, K., Chikae, M., Kim, D.-K., Yamamura, S., Tamiya, E. (2007). A localized surface plasmon resonance based immunosensor for the detection of casein in milk. Science and Technology of Advanced Materials, 8(4), 331-338.

Montojo, J., Zuberi, K., Rodriguez, H., Bader, G. D., & Morris, Q. (2014). GeneMANIA: fast gene network construction and function prediction for Cytoscape. F1000Research, 3.

Mori, K. (2009). Signalling pathways in the unfolded protein response: development from yeast to mammals. Journal of biochemistry, 146(6), 743-750.

Nagai, T., Ibata, K., Park, E. S., Kubota, M., Mikoshiba, K., & Miyawaki, A. (2002). A variant of yellow fluorescent protein with fast and efficient maturation for cell-biological applications. Nature biotechnology, 20(1), 87-90.

Nojima, H., Leem, S.-H., Araki, H., Sakai, A., Nakashima, N., Kanaoka, Y., & Ono, Y. (1994). Hac1: A novel yeast bZIP protein binding to the CRE motif is a multicopy suppressor for cdcW mutant of Schizosaccharomyces pombe. Nucleic acids research, 22(24), 5279-5288.

Patil, C., & Walter, P. (2001). Intracellular signaling from the endoplasmic reticulum to the nucleus: the unfolded protein response in yeast and mammals. Current opinion in cell biology, 13(3), 349-355.

Patil, C. K., Li, H., & Walter, P. (2004). Gcn4p and novel upstream activating sequences regulate targets of the unfolded protein response. PLoS biology, 2(8), e246.

Pavitt, G. D., Ramaiah, K. V., Kimball, S. R., & Hinnebusch, A. G. (1998). eIF2 independently binds two distinct eIF2B subcomplexes that catalyze and regulate guanine–nucleotide exchange. Genes & development, 12(4), 514-526.

Pfleger, K. D., & Eidne, K. A. (2006). Illuminating insights into protein-protein interactions using bioluminescence resonance energy transfer (BRET). Nature methods, 3(3), 165-174.

Phizicky, E. M., & Fields, S. (1995). Protein-protein interactions: methods for detection and analysis. Microbiological reviews, 59(1), 94-123.

Pollok, B. A., & Heim, R. (1999). Using GFP in FRET-based applications. Trends in cell biology, 9(2), 57-60.

Rubio, C., Pincus, D., Korennykh, A., Schuck, S., El-Samad, H., & Walter, P. (2011). Homeostatic adaptation to endoplasmic reticulum stress depends on Ire1 kinase activity. The Journal of cell biology, 193(1), 171-184.

Sherman, F. (2002). Getting started with yeast. Methods in enzymology, 350, 3-41.

Sung, M.-K., Lim, G., Yi, D.-G., Chang, Y. J., Yang, E. B., Lee, K., & Huh, W.-K. (2013). Genome-wide bimolecular fluorescence complementation analysis of SUMO interactome in yeast. Genome research, 23(4), 736-746.

Tajika, Y., Sakai, N., Tamura, T., Yao, M., Watanabe, N., & Tanaka, I. (2005). Crystal structure of PH0010 from Pyrococcus horikoshii, which is highly homologous to human AMMECR 1C-terminal region. Proteins: Structure, Function, and Bioinformatics, 58(2), 501-503.

Tarassov, K., Messier, V., Landry, C. R., Radinovic, S., Molina, M. M. S., Shames, I., Michnick, S. W. (2008). An in vivo map of the yeast protein interactome. Science, 320(5882), 1465-1470.

Teske, B. F., Wek, S. A., Bunpo, P., Cundiff, J. K., McClintick, J. N., Anthony, T. G., Wek, R. C. (2011). The eIF2 kinase PERK and the integrated stress response facilitate activation of ATF6 during endoplasmic reticulum stress. Molecular biology of the cell, 22(22), 4390-4405.

Travers, K. J., Patil, C. K., Wodicka, L., Lockhart, D. J., Weissman, J. S., & Walter, P. (2000). Functional and genomic analyses reveal an essential coordination between the unfolded protein response and ER-associated degradation. Cell, 101(3), 249-258.

Uetz, P., Giot, L., Cagney, G., Mansfield, T. A., Judson, R. S., Knight, J. R., Pochart, P. (2000). A comprehensive analysis of protein–protein interactions in Saccharomyces cerevisiae. Nature, 403(6770), 623-627.

Vitelli, F., Piccini, M., Caroli, F., Franco, B., Malandrini, A., Pober, B., Renieri, A. (1999). Identification and characterization of a highly conserved protein absent in the Alport syndrome (A), mental retardation (M), midface hypoplasia (M), and elliptocytosis (E) contiguous gene deletion syndrome (AMME). Genomics, 55(3), 335-340.

Warde-Farley, D., Donaldson, S. L., Comes, O., Zuberi, K., Badrawi, R., Chao, P., Lopes, C. T. (2010). The GeneMANIA prediction server: biological network integration for gene prioritization and predicting gene function. Nucleic acids research, 38(suppl 2), W214-W220.

Xu, Y., Piston, D. W., & Johnson, C. H. (1999). A bioluminescence resonance energy transfer (BRET) system: application to interacting circadian clock proteins. Proceedings of the National Academy of Sciences, 96(1), 151-156.

Yang, M., Wu, Z., & Fields, S. (1995). Protein-peptide interactions analyzed with the yeast two-hybrid system. Nucleic acids research, 23(7), 1152-1156.

국문초록

단백질의 대부분의 세포 내 기능은 다른 단백질들과의 상호작용에 의해 이루어 지기 때문에, 단백질의 기능을 밝히는데 그 단백질의 상호작용을 확인하는 것은 중요하다. 이러한 이유로 어느 단백질의 인터랙톰을 알 수 있다면, 그 단백질의 기능을 알아낼 수 있다. 본 연구에서 효모의 전체 단백질에 대하여 이분자 형광 상보 (BiFC) 스크리닝 기법을 사용해 기능이 알려지지 않은 단백질인 Yor289w와 상호작용하는 효모 단백질들의 후보군 들을 확인하였다. pRPL7B-VN-YOR289W 균주와 VC 융합 라이브러리 균주들을 각각 교배 후 일련의 가짜 형광신호를 제거하는 과정을 거쳐 56개의 Yor289w와 상호작용 할 것으로 생각되는 후보군들을 얻을 수 있었다. 이 인터랙톰의 분석 결과 후보군들이 translation initiation and nucleobase-containing small molecule metabolic processes 등의 세포 내 작용에 관련이 있는 것으로 확인되었다. 이후 Yor289w 단백질의 발현량이 unfolded protein response (UPR) 상황에서 증가하는 것을 확인하였다. 그리고 이러한 단백질의 증가양상이 UPR의 중요 조절인자인 Hac1과 Ire1 에 의존적이라는 사실을 확인하였다. 이러한 Yor289w의 발현양상은 이 단백질이 Hac1과 Ire1에 의해 직접 조절된다는 것을 의미한다. 일련의 전체 효모 단백질을 대상으로 한 이분자 형광 상보 스크리닝과 Yor289w의 단백질 발현양상을 확인하는 과정을 통해, Yor289w가 UPR 상황에서 번역조절에 관여할 수 있다는 가능성을 확인할 수 있었다.

주요어: YOR289W, 단백질 상호작용, BiFC 기법, *Saccharomyces cerevisiae*, Unfolded protein response (UPR)